

Role of Ion Orbit Loss of Thermalized Ions in the Edge Plasma in Determining the Radial Electric Field in the Tokamak Edge Plasma

Weston M. Stacey

weston.stacey@nre.gatech.edu

Georgia Institute of Technology

Atlanta, GA 30332, USA

ABSTRACT Differences in the radial electric field in the plasma edge are observed to be associated with significantly different plasma confinement. This poster examines the role that the kinetic ion orbit loss of the outflowing thermalized plasma ions and the compensating inward thermalized ion current required for charge neutrality play in creating the rather unique structure of the radial electric field in tokamak edge plasmas. The basic physical mechanisms considered are 1) the ion orbit loss of thermalized ions, 2) the compensating inward transport of particles and of poloidal momentum by a) the viscous inward transport of ions and b) the inward recycling of neutral atoms to the edge plasma from the scrape-off layer to provide a compensating inward radial current of ions in the edge plasma to offset the ion orbit loss and maintain charge neutrality, and 4) the consequential resetting of the edge plasma radial electric field to maintain momentum balance in the presence of such particle currents. The resulting theory compares qualitatively with experimental measurements of the radial electric field in the plasma edge.

Sherwood Theory Mtg 2018

Auburn, AL April 23-25, 2018

ION ORBIT LOSS

The ion orbit loss of outflowing thermalized ions in the tokamak edge plasma which are able to access drift orbits that carry them outward across the separatrix and into the scrape-off layer (SOL) or divertor produces an outward IOL ion current that must be compensated by an inward ion current to maintain charge neutrality. It is proposed in this poster that the currents arising to compensate for ion orbit loss in part determine the radial electric field in the tokamak edge plasma.

There is the minimum speed, $V_{0\min}(\zeta_0)$, for which an outflowing thermalized ion at a given location on an internal flux surface with direction cosine ζ_0 (with respect to \mathbf{B}) can reach a given location on the last closed flux surface (LCFS). This quantity can be determined^{3,7} from conservation of canonical angular momentum, energy and magnetic moment, which yield an equation for this minimum value of the escape speed $V_0(\psi, \theta, \zeta_0)$

$$V_0^2 \left[\left(\frac{R_0}{R} \frac{f_{\phi 0}}{f_\phi} \zeta_0 \right)^2 - 1 + (1 - \zeta_0^2) \left| \frac{B}{B_0} \right| \right] + V_0 \left[\frac{2e(\psi_0 - \psi)}{Rmf_\phi} \left(\frac{R_0}{R} \frac{f_{\phi 0}}{f_\phi} \zeta_0 \right) \right] + \left[\left(\frac{e(\psi_0 - \psi)}{Rmf_\phi} \right)^2 - \frac{2e(\phi_0 - \phi)}{m} \right] = 0 \quad (1)$$

ION ORBIT LOSS FRACTION

The fraction of the outflowing thermalized ion flux that is in the form of ion orbit loss particles free-streaming outward across an internal flux surface are the fractions of these distributions associated with particles with energies greater than the minimum loss energy (or speed), $V_0(\rho, \zeta_0) > V_{0\min}(\rho, \zeta_0)$,

$$\begin{aligned}
 F_{IOL} &\equiv \frac{n_{loss}}{n_{tot}} = \frac{\int_{-1}^1 \left[\int_{V_{0\min}(\zeta_0)}^{\infty} R_{loss}^{iol}(V_0, \zeta_0) f(V_0) V_0^2 dV_0 \right] d\zeta_0}{\int_{-1}^1 \left[\int_0^{\infty} f(V_0) V_0^2 dV_0 \right] d\zeta_0} \\
 &= \frac{1}{2} \int_{-1}^1 \left\langle R_{loss}^{iol}(V_{0\min}(\zeta_0), \zeta_0) \right\rangle_n \left[\frac{\Gamma(3/2, \varepsilon_{\min}(\zeta_0))}{\Gamma(3/2)} \right] d\zeta_0 \quad (2)
 \end{aligned}$$

where R_{loss}^{iol} is the fraction of such particles leaving the confined plasma that do not return into the plasma, $\varepsilon_{\min} \equiv mV_{0\min}^2(\zeta_0)/2T$, Γ is the gamma function and a Maxwellian distribution has been used to evaluate the integrals over ion speed. for an ion with a given speed (V_0) and direction cosine ξ_0 located at a given position on an internal flux surface ψ_0 being able to access a loss orbit that crosses the LCFS $\psi(x)$ at a given location x , where $\phi(\psi)$ is the electrostatic potential and $f_\phi \equiv |B_\phi/B|$.

CUMULATIVE ION ORBIT LOSS IN MATCHED H-MODE & RMP SHOTS IN DIII-D

Figures 1 indicate that the local ion orbit loss rate becomes quite large for $\rho > 0.96$.

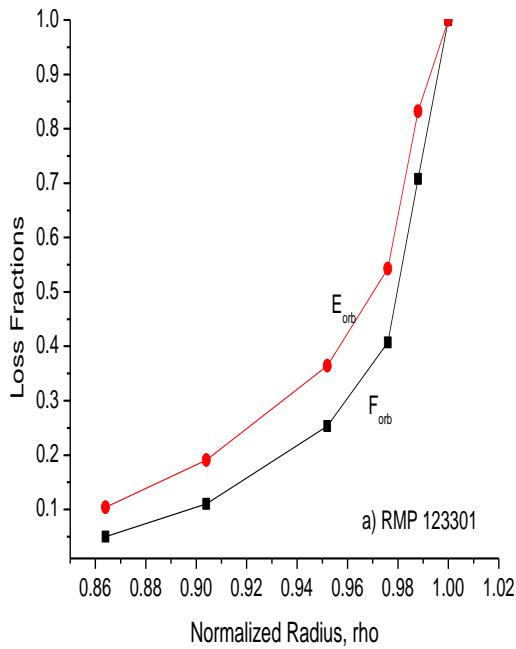


Fig. 1a IOL Ion F^{IOL} and Energy E^{IOL} Loss Fractions for RMP Shot

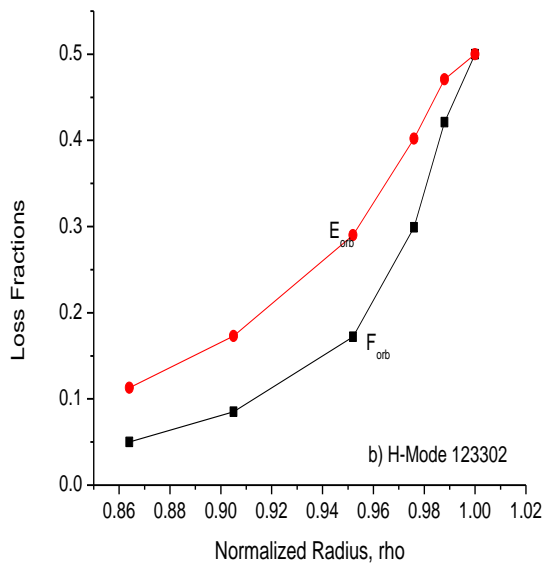


Fig. 1b IOL Ion and Energy Loss Fractions for H-mode Shot

The much larger ion orbit loss rate for RMP than H-mode is consistent with the “density pumpout” effect of RMP.

INCLUSION OF ION ORBIT LOSS INTO FLUID EQUATIONS

The $F_{iol}(\rho, \zeta_0, \theta_0, \theta_s)$ are calculated at a number of poloidal locations θ_0 on the internal flux surface and θ_s on the LCFS, and are appropriately averaged^{7,15} to obtain a value characterizing the internal flux surface at radius ρ_0 . **These factors are incorporated into the fluid continuity equation as differential losses proportional to the radial particle fluxes¹⁷**

$$\frac{1}{r} \frac{\partial r \Gamma_{ri}}{\partial r} = -\frac{\partial n_i}{\partial t} + N_{nbi} (1 - 2f_{nbi}^{iol}) + n_e v_{ion} - 2 \frac{\partial F_{IOLi}}{\partial r} \Gamma_{ri} \quad (3)$$

Making use of the method of integrating factors, it can be shown that Eq. (3) has solutions of the form

$$r \Gamma_{ri}(r) = r_0 \Gamma_{ri}(r_0) + \int_{r_0}^r r' S_{ni}(r') e^{-2[F_{IOLi}(r) - F_{IOLi}(r')]} dr' \quad (4)$$

The kinetic loss of ions by IOL constitutes a radially outward kinetic IOL ion current in the plasma edge

$$J_{rIOL}(r) = \frac{1}{r} \int_0^r \left[e_j N_{nbj}(r') f_{nbj}^{IOL}(r') + e_j \frac{\partial F^{IOLj}(r')}{\partial r'} \Gamma_{rj}(r') + e_k \frac{\partial F^{IOLk}(r')}{\partial r'} \Gamma_{rk}(r') \right] r' dr' \quad (5)$$

COMPENSATING RETURN CURRENT CONTRIBUTIONS FROM PLASMA EDGE & SOL

A. Inward Current Of Thermalized Ions Driven By Inward Viscous Transport Of Strongly Rotating Ions Across Separatrix

Both measurements (e.g. Ref. 19) and theoretical modeling (e.g. Ref. 20) of diverted tokamaks show that the carbon and deuterium plasma species flow in the SOL at similar, near-sonic magnitude toward the divertor plates and have a stagnation point between divertor plates. Other theoretical calculations predict a viscous radially inward flow of ions with large poloidal momentum from the SOL into the plasma edge²¹ for a DIII-D H-mode plasma. Such an ion poloidal momentum source into the edge plasma could drive a radially inward ion current via the radial momentum balance $\langle (J \times B)_\theta \rangle_{visc} = (J_r^{visc} B_\phi) = -\langle n_i m_i v_{visc} V_{i\theta} \rangle$ in the plasma edge, where v_{visc} is a representative inward viscous momentum transport frequency from the SOL into the plasma edge that could be calculated using e.g. Ref.21 or a more rigorous model taking into account toroidal non-axisymmetry²².

B. Inward Current Of Thermalized Ions Driven By Neutral-Ion Momentum Exchange In The Plasma Edge

Neutral atoms from edge recycling or gas fueling are present in the SOL and edge plasma of tokamaks, due to the recycling of ions from the chamber wall and to gas fueling. These neutral atoms are primarily directed inward and transport poloidal momentum acquired in the SOL into the edge plasma. The poloidal momentum exchange from neutral atoms to ions in the edge plasma, averaged over a $0-2\pi$ gyro-orbit, can drive an inward radial current of thermalized ions, $J_{in} = -J_{IOL}$, via the poloidal ion momentum balance equation
 $\langle (J \times B)_\theta \rangle_{neut} = \langle (J_r B_\phi) \rangle_{neut} = \langle n_i m_i v_{i-n} (V_{n\theta} - V_{i\theta}) \rangle^{23,24}$. The collision frequency ν_{i-n} includes charge-exchange and elastic scattering of ions and neutrals. The $\langle \rangle$ indicates a $0-2\pi$ orbit average over the ion gyro-orbit, taking into account variations in ion velocity due to $E \times B$ and diamagnetic drifts, and variations in the neutral velocity (V_n) direction and density (n_n). This concept is discussed in detail in Refs. 23 and 24; charge exchange is emphasized, but the momentum transfer process generalizes to all neutral-ion interactions that transfer momentum. The basic argument is that when there is an asymmetry in the ion-neutral relative velocity and the neutral density varies around the ion rotation orbit about the magnetic field, net ion motion in the poloidal direction occurs, which generates a radial current. The neutral density increases strongly with increasing radius in the plasma edge. The resulting expression (taking into account ExB and diamagnetic ion drifts and the neutral density variation with radius) for the radial component of the ion current due to incoming neutrals is

$$J_r^{neut} = \frac{n_i m_i \nu_{in} n_n}{B_\phi} \left(\frac{E_r}{B_\phi} - \frac{\nabla p_i}{e_i B_\phi n_i} + \frac{kT_i \nabla n_n}{e_i B_\phi n_n} \right) \quad (6)$$

RADIAL ELECTRIC FIELD TO SATISFY RADIAL MOMENTUM BALANCE

Setting $J_r^{neut} + J_r^{visc} = -J_{rIOL}$ from Eq. (5), Eq. (6) can be solved for the radial electric field required for charge neutrality in the presence of ion orbit loss.

$$\frac{E_r}{B} = \frac{-(J_{rIOL} + J_r^{visc})B}{e_i n_i v_{i-n} n_n} + \frac{\nabla p_i}{e_i n_i} - \frac{kT_i \nabla n_n}{e_i B n_n} \quad (7)$$

All three terms on the right in Eq. (7) are < 0 in the edge plasma of tokamaks, since $J_{rIOL} > 0$, $\nabla p_i < 0$, $\nabla n_n > 0$. Ion orbit loss, and hence J_{rIOL} , are negligible over most of the plasma, but increase dramatically in the outer 10% in radius to just less than 100% of the outflowing ions. The last two terms are large just inside the last closed flux surface (LCFS) where the ion pressure gradient is large and negative and the neutral density gradient is large and positive. Both J_{rIOL} and n_n are largest just inside the LCFS and decrease inward towards the plasma core.

RELATION TO TOKAMAK EXPERIMENTAL OBSERVATIONS

In this section we relate the above theoretical considerations to measurements from the DIII-D tokamak²⁵. Results from a standard H-mode discharge (#123302) and a similar discharge with Resonance Magnetic Perturbation (RMP) coils turned on (#123301) but otherwise operated identically, are considered. All figures are from Ref. 7 .

The measured edge electron density (similar to the ion deuterium density), ion temperature (T_i), and electrostatic potential (ϕ) in the edge plasma of the H-mode discharge are shown in Fig. 2. For the RMP discharge the electron (and ion) density was significantly lower, and consequently the ion temperature was substantially larger, as shown in Fig. 3.

The measured electric field shown in Fig 4 is somewhat more negative in the H-mode than in the RMP discharge. This is consistent with Eq. (7) showing that the electric field magnitude is proportional to the IOL current and the larger calculated IOL loss for the H-mode than for the RMP discharge shown in Fig. 4.

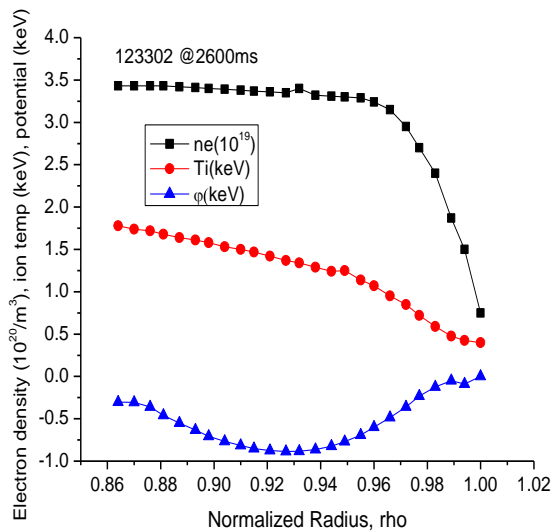


Fig. 2 Measured Edge n_e , T_i and ϕ H-mode

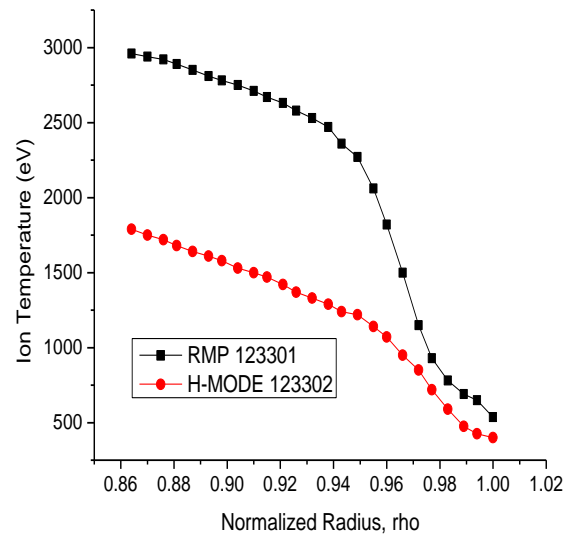


Fig. 3 Ion Temperature in RMP and in H-mode.

MEASURED ELECTRIC FIELD

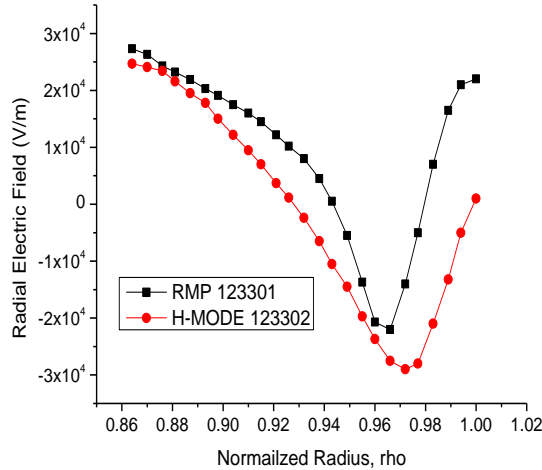


Fig. 4 Measured Electric Field in Plasma Edge

The ion orbit particle loss calculated from Eq. (1) for the RMP discharge was significantly larger than the loss for the H-mode discharge, as shown in Fig. 1. (A similar calculation of ion orbit energy loss is also shown.) Note that $F^{IOL}(r)$ is the cumulative ion orbit loss over $0 < r' < r$, so that $\partial F^{IOL}(r)/\partial r$ is the local differential ion orbit loss rate coefficient at location r .

RADIAL ELECTRIC FIELD PROFILE MATCHES ION ORBIT DIFFERENTIAL LOSS RATE

Note that the normalized radii where the differential particle loss rates $\frac{\partial F_j^{IOL}(r')}{\partial r'} \Gamma_{ij}(r')$ are largest in Figs. 1 correspond to the location of the wells (largest negative value) in the measured electric fields shown in Fig. 4, suggestive of the type of relationship between ion orbit loss and the radial electric field discussed above in this poster.

SUMMARY

This poster examines the concept that ion orbit loss of thermalized ions and the return currents necessary to maintain plasma neutrality could be significantly responsible for the rather unique structure of the radial electric field in the edge of tokamak plasmas. The basic mechanism involved is the establishment of a compensating inward radial current of ions in the edge plasma to maintain charge neutrality against the ion orbit loss, and the resetting of the radial electric field to maintain momentum balance in the presence of such an inward ion current in the plasma. The model used in this poster, in which the compensating ion return current is driven by poloidal momentum exchange to ions in the edge plasma from recycling neutrals and from the SOL ions viscously transported inward across the separatrix, is shown to be qualitatively consistent with experimental observations in DIII-D. This result is suggestive that control of the ion orbit loss and/or the compensating return current could be a way to control the electric field in the edge plasma, hence to control plasma confinement. Further theoretical and experimental investigation are obviously needed.

Email Signup Sheet

REFERENCES

1. F. L. Hinton and M. Chu, Nucl. Fusion 25, 345 (1985).
2. A. Chankin and G. McCracken, Nucl. Fusion 33, 1459 (1993).
3. K. Miyamoto, Nucl. Fusion 36, 927 (1996).
4. G. F. Mathews, G. Corrigan, S. K. Erents. W. Fundamenski, A. Kallenbach, T. Kirki-Suonio, S. Sipila and J. Spence, JET Report EFDA-JET-CP(02)01 (2002).
5. N. Axarenkov and Zh. Kononenko, J. Kharkiv Univ. 859, 51 (2009).
6. J. S. deGrassie, R. J. Groebner, K. H. Burrell and W. M. Solomon, Nucl. Fusion 49, 085020 (2009).
7. W. M. Stacey, Phys. Plasmas 18, 102504 (2011).
8. C. S. Chang, S. Kue and H. Weitzner, Phys. Plasmas 9, 3884 (2002).
9. C. S. Chang, S. Kue and H. Weitzner, Phys. Plasmas 11, 2649 (2004).
10. H. Weitzner and C. S. Chang, Phys. Plasmas 11, 3060 (2004).
11. C. S. Chang, Phys. Plasmas 11, 5626 (2004).
12. W. M. Stacey, Phys. Plasmas 18, 122504 (2011).
13. W. M. Stacey, J. A. Boedo, T. E. Evans, B. A. Grierson and R. J. Groebner, Phys. Plasmas 19, 112503 (2012).
14. W. M. Stacey and B. A. Grierson, Nucl. Fusion 54, 073021 (2014).
15. W. M. Stacey and M. T. Schumann, Phys. Plasmas 22, 042504 (2015).
16. T. M. Wilks and W. M. Stacey, Phys. Plasmas 23, 122505 (2016).
17. W. M. Stacey and T. M. Wilkes, Phys. Plasmas 23, 012508 (2016).
18. W. M. Stacey, Nucl. Fusion 57, 066034 (2017).
19. M. Groth, G. D. Porter, J. A. Boedo, et al, J. Nucl. Mat. 390-391, 343 (2009).
20. W. M. Stacey, Phys. Plasmas 16, 032506 (2009).
21. W. M. Stacey, Phys. Plasmas 16, 062505 (2009).
22. W. M. Stacey and C. Bae, Phys. Plasmas 062503 (2015).
23. K. C. Lee, Phys. Plasmas 13, 062505 (2006).
24. K. C. Lee, Phys. Plasmas 24, 112505 (2017).
25. J. Luxon, Nucl. Fusion 42, 614 (2002).